PHILOSOPHICAL TRANSACTIONS OF THE ROYAL SOCIETY A MATHEMATICAL, PHYSICAL & ENGINEERING SCIENCES

High-Energy Short-Pulse Carbon Dioxide Lasers [and Discussion]

C. Fenstermacher and C. Yamanaka

Phil. Trans. R. Soc. Lond. A 1980 **298**, 377-391
doi: 10.1098/rsta.1980.0261

Phil. Trans. R. Soc. Lond. A **298**, 377–391 (1980)
Printed in Great Britain

High-energy short-pulse carbon dioxide lasers

By C. Fenstermacher
Laser Research and Technology Division, Los Alamos Scientific Laboratory, Los Alamos, New Mexico 87545, *U.S.A.*

Lasers for fusion application represent a special class of short-pulse generators: not only must they generate extremely short temporal pulses of high quality, but they must do this at ultra-high powers and satisfy other stringent requirements. This paper presents the status of the research and development of carbon dioxide laser systems at the Los Alamos Scientific Laboratory, *vis-à-vis* the fusion requirements.

1. Fusion laser requirements

Because one is seeking the highest attainable optical intensity on the microsphere target in a subnanosecond pulse, fusion lasers operate in the so-called oscillator–amplifier configuration shown in figure 1.

The fusion laser system requirements can be stated in reference to this configuration.

1. The lasing medium for the amplifier stages must be capable of efficiently storing optical energy at high densities so that machines are of a feasible size.

2. The oscillator should be capable of generating the prescribed shape in short, subnanosecond pulses with good contrast ratio, that is, a high ratio of main pulse energy to background to avoid prepulse target damage.

3. The laser medium should have adequate optical gain coefficient to provide efficient extraction of the stored energy by the oscillator pulse.

4. The energy storage and short-pulse extraction should result in overall system efficiencies of 5 to 10 %.

5. A single amplifier chain should be capable of repetitively pulsed outputs with the single-pulse output in the several kilojoule range so that the number of individual beams can be kept to a reasonable number at the 100 kJ to 1 MJ level.

2. CO_2 laser fundamentals

Witteman (1966) and Moore *et al.* (1967) have provided comprehensive treatments of the various aspects of the basic CO_2 laser phenomena and a detailed description of the molecular kinetics of this system's energy levels can be found in De Maria (1976), one of the most recent discussions of this laser. The CO_2 laser operates on a population inversion between the first vibrational states of the antisymmetric and symmetric stretch modes of the molecule as indicated in figure 2. A third vibrational mode, the bending mode, provides a path for collisional deactivation of the lower lasing level. Excitation of the upper vibrational level can be achieved by thermal, chemical, optical and electrical pumping. However excited, the energy of this level is distributed over a manifold of rotational sublevels according to a Boltzmann distribution function, giving rise to the possibility of many lasing transitions between the two vibrational

levels. Figure 3 schematically illustrates two allowed optical transitions. From symmetry consideration on the total wavefunction for the normal CO_2 molecule, only odd values of rotational angular momentum, j, exist for the upper vibrational laser state and only even values exist for the lower laser level. Transitions between the two levels with $\Delta j = \pm 1$ are allowed and are denoted as P and R transitions respectively, the final j value being designated for a given transition, for example P(20) indicates the $\Delta j = +1$ transition from $j = 19$ to $j = 20$.

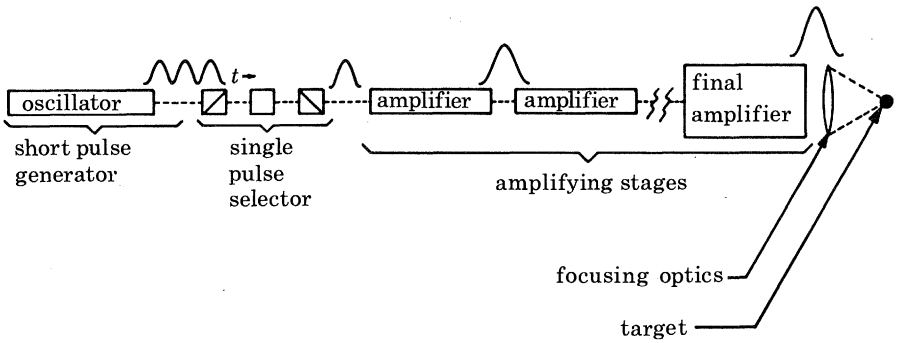

FIGURE 1. Oscillator–amplifier configuration used for high-energy, short-pulse fusion lasers. Pulse amplifications are typically 10^6 in such systems.

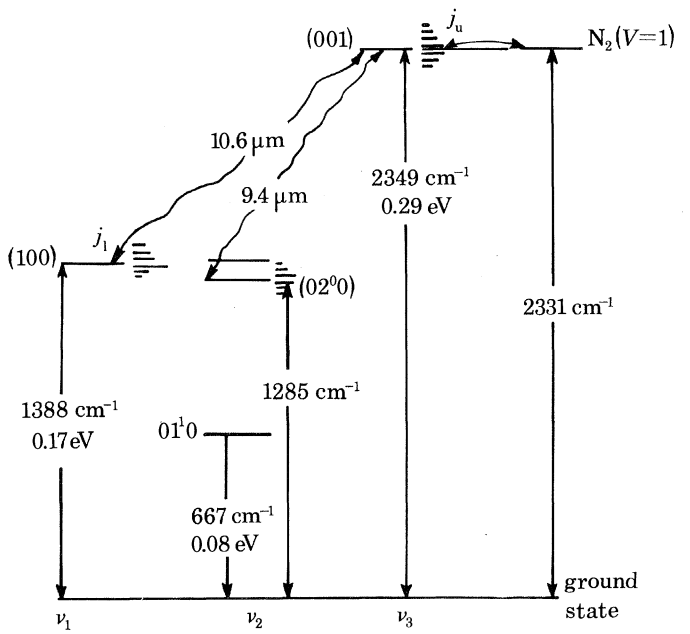

FIGURE 2. CO_2 laser energy level diagram. Pumping is by direct excitation of the (001) level and excitation of the N^2 ($V = 1$) level with subsequent collisional energy transfer. Transitions between the (001) upper level and the (100) and (020) levels produce lasing over a band from 9 to 11 μm.

Based upon consideration of optical energy storage or 'gain storage', electrical pumping has been found to be the most efficient and scalable process. In electrically pumped CO_2 lasers, the upper levels are excited by inelastic electron–molecule collisions. The process is represented by

$$CO_2(0, 0, 0) + e(\epsilon_k) \rightarrow CO_2^*(\nu_1, \nu_2, \nu_3), \quad (1)$$

where (ν_1, ν_2, ν_3) indicates the levels excited for the three vibrational modes, $(0, 0, 0)$ being the ground state and ϵ_k the electron energy. The excitation rate of the various levels is a strong function of the electron energy, which in turn depends upon the discharge electric field: molecular density ratio, $E{:}N$, and it is discussed below.

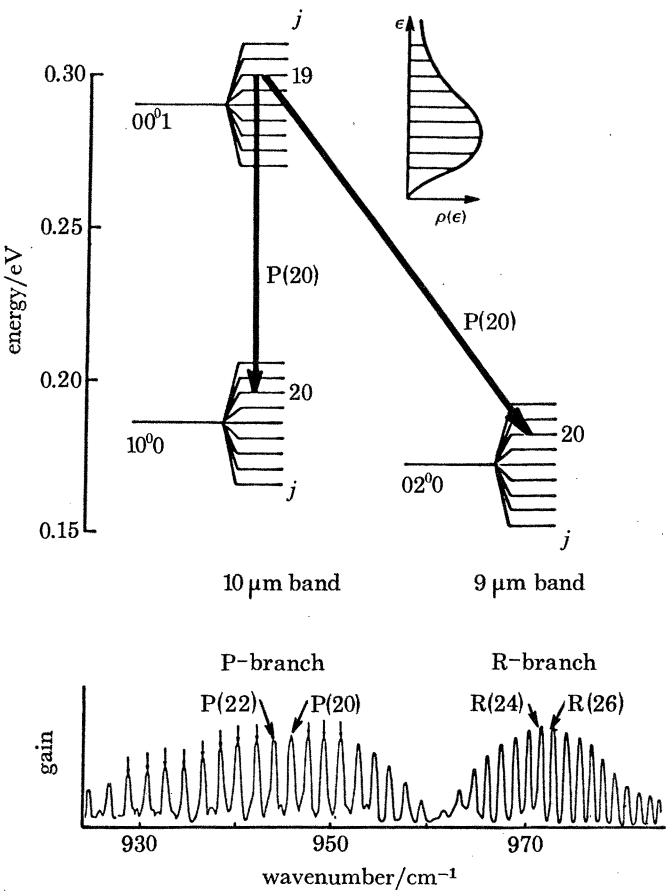

FIGURE 3. Lasing transitions in 9 and 10 μm bands of CO_2 (upper) and spectrum of P and R branch of 10 μm band (lower).

3. PUMPING MECHANISM, OPTICAL GAIN AND ENERGY STORAGE

Consideration of the fundamentals indicates that for a high-energy short-pulse CO_2 fusion laser one must seek a high-pressure, large volume, uniform discharge in which the electrical and gas parameters can be controlled. In 1969 a technique to produce such a discharge based upon the electron-beam controlled discharge was conceived independently at both the Avco Everett Research Laboratory (Daugherty *et al.* 1972) and at the Los Alamos Scientific Laboratory (Fenstermacher *et al.* 1971, 1972). All large CO_2 fusion lasers at Los Alamos use this technique, which we now describe.

High-pressure, self-sustained gaseous electrical discharges are inherently unstable and quickly degenerate into constricted, low-impedance arcs, which are unsuitable for efficient volumetric laser pumping. The electron-beam controlled discharge technique avoids such instability problems by decoupling the charge production in the discharge from the electric

field, thus allowing a discharge to be produced at field strengths that do not require secondary electron multiplication or avalanching, a source of instabilities. The separation of charge production from the electric field is done by the use of a high-energy electron beam as an external ionizing agent. The apparatus used in this technique is illustrated in figure 4. A voltage less than the breakdown value of the gas is applied to the electrodes, and high-energy electrons from an electron gun operating in a vacuum are injected into the gas discharge volume through a thin metal foil. The secondary electrons produced in the gas by this external ionizing source act as the current carriers in the gas, producing an ohmic or linear discharge. For a secondary electron production rate in the gas volume, S (electrons $\mathrm{cm}^{-3}\,\mathrm{s}^{-1}$), and an electron loss rate,

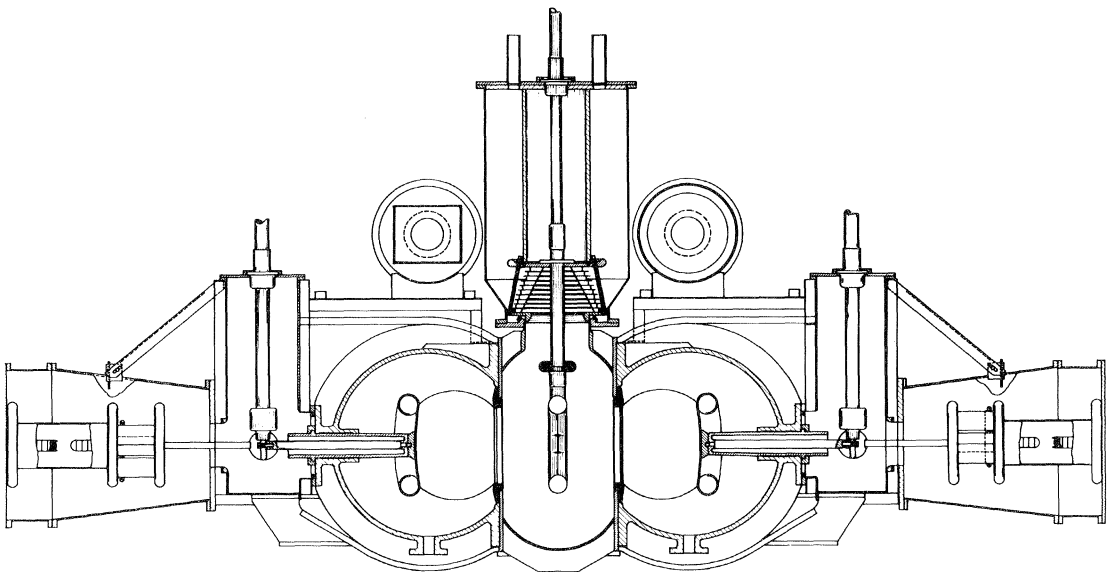

FIGURE 4. Cross section of a dual electron beam-controlled CO_2 laser. The two-sided, common, cold-cathode electron gun supplies electrons to ionize both laser discharge cavities. The main discharge is created between cathode and anode of the laser cavities.

α, due to volume recombination, the discharge is modelled quite well by the following simple equations relating electron and ion number density, n_e, n_i current flow, j, and electron drift velocity, v_d:

$$\mathrm{d}n_e/\mathrm{d}t = S - \alpha n_i n_e = S - \alpha n_e^2, \quad n_i = n_e. \tag{2}$$

With S taken as a step function in time, the equation integrates simply:

$$n = n_0 \tanh (\alpha S)^{\frac{1}{2}} t \quad S = S_0, \quad 0 < t < t_0 \tag{3}$$

$$= \frac{n_0}{1 + n_0 \alpha t}; \qquad S = 0, \quad t > t_0, \tag{4}$$

with $n_0 = (S/\alpha)^{\frac{1}{2}}$. The current density, j, in the presence of the applied field, E, is

$$j = n_e e v_d \tag{5}$$

and the volumetric power density in the gas, w, is

$$w = Ej = En_e e v_d. \tag{6}$$

For cases of interest, the primary ionizing energy is relatively small, about 1–2% of the main discharge energy.

This process has been well studied (Basov *et al.* 1975; Leland 1976). The work at Los Alamos has shown this to be a feasible technique that can be scaled to the levels needed for the laser-fusion application.

The results of parametric studies of the pumping process are given in figure 5, which shows the dependence of optical gain on the energy input.

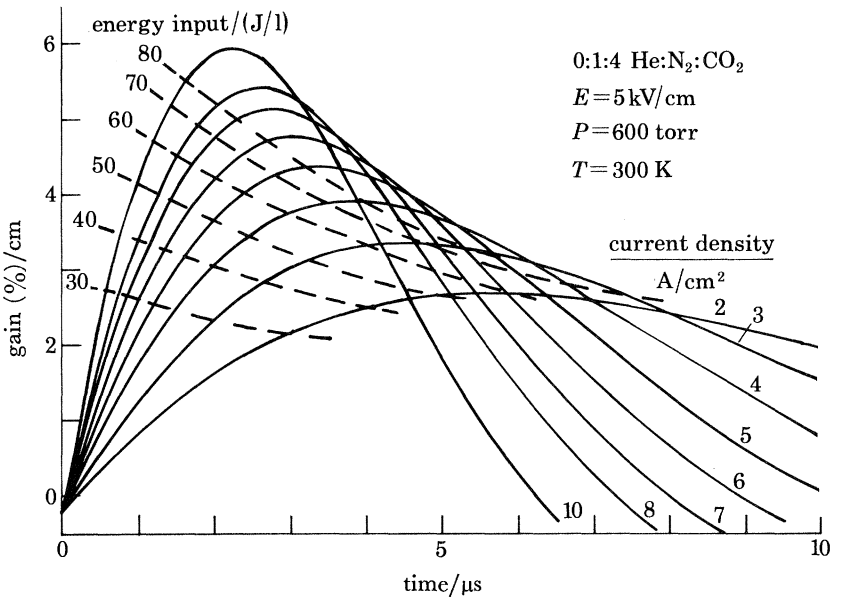

FIGURE 5. Optical gain plotted against time for varying energy input.

The optical gains shown are measured on the P(20) transition at line centre, and for the homogeneously pressure-broadened region are related to the population of the $j = 19$ upper level and $j = 20$ lower level by

$$g_0 = \frac{\lambda^2}{4\pi^2 \tau_s \Delta\nu}\left(n_{19} - \frac{g_{19}}{g_{20}} n_{20}\right), \tag{7}$$

in which g_0 is the optical gain coefficient (cm^{-1}), λ the wavelength, $\Delta\nu$ the full width at half maximum for the transition, τ_s the radiative lifetime of the transition, and n_{19}, n_{20} the upper and lower level populations, g_{19}, g_{20} being their statistical weights. The P(20) transition lies at or near the maximum of the rotational population distribution over the temperature range of interest (350–400 K).

The population inversion of the P(20) transition represents about 6% of the total inversion. Optical energy storage densities of 10 J/l atmosphere have been obtained.

4. SHORT PULSE GENERATION

In the first CO_2 fusion laser systems, mode-locking was used to generate the master pulse. Subnanosecond pulse generation by mode-locking implies operation at very high pressures. A reduction by a factor of three in pulse width to not more than 0.3 ns requires operation at approximately 10 atm (*ca.* 1 MPa). Such operation can be achieved, but involves higher

voltage discharges and more complications than necessary. Subnanosecond pulses can be produced with oscillators operating at atmospheric pressure with more conventional discharge circuits by applying the modulation at the output by using electro-optic shutters to slice out a short pulse. The bandwidth of the medium becomes irrelevant in this case.

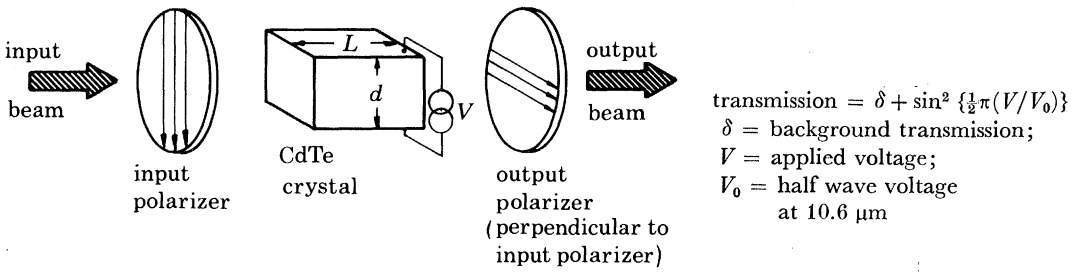

FIGURE 6. Principle of electro-optic shutter used for short pulse generation. The time history of the applied voltage determines the pulse shape.

Electro-optic shutters are based upon the use of optically active crystals that become birefringent upon the application of electric fields (Walsh 1966). The materials of choice for 10.6 μm optical modulation are single crystal gallium arsenide or cadmium telluride. The use of an electro-optic shutter to generate a short pulse is shown schematically in figure 6. With fast rising voltage pulses applied to three electro-optic switches in series, pulses as short as 150 ps have been generated.

Single-stage electro-optic switches can provide contrast ratios of 500–1000, the limit being set largely by the uniformity of the birefringence of the electro-optic crystal. By staging several switches, contrast ratios of 10^7–10^8 have been attained. The additional contrast ratio required is obtained through the use of saturable absorbers, i.e. absorbers that show marked nonlinear transmission as a function of intensity.

5. SHORT PULSE AMPLIFICATION

The theory of pulse propagation through a two-level laser amplifier has been well developed (Frantz & Nodvik 1963; Kryukov & Letokhov 1970). With modification, these results can be applied to the multilevel CO_2 laser (Schappert 1973). In the Frantz–Nodvik treatment, solutions to the photon transport equations are derived for the amplification of specific pulse shapes, e.g. square and Lorentzian shape, as well as for the general case. The essentials are summarized here.

The two-level photon transport equation for an amplifying volume is

$$\partial n/\partial t + c(\partial n/\partial x) = \sigma c n(N_2 - N_1), \tag{8}$$

with $n(x, t)$ the photon density, c the velocity of light, σ the stimulated emission cross section, and N_2, N_1 the upper and lower laser state population densities.

The associated equations on population inversion are

$$\left.\begin{aligned} \partial N_1/\partial t &= \sigma c n(N_2 - N_1), \\ \partial N_2/\partial t &= -\sigma c n(N_2 - N_1), \end{aligned}\right\} \tag{9}$$

which, together with (8), define the two-level system. By setting $\Delta = N_2 - N_1$ these can be rearranged:

$$\left.\begin{aligned} \partial n/\partial t + c\partial n/\partial x &= \sigma c n \Delta, \\ \partial \Delta/\partial t &= -2\sigma c n \Delta, \end{aligned}\right\} \tag{10}$$

with general solution

$$\left.\begin{aligned} n(x,t) &= \frac{n_0(t-x/c)}{1-\left\{1-\exp\left[-\sigma\int_0^x \Delta_0(x')\,\mathrm{d}x'\right]\right\}\exp\left[-2\sigma c\int_{-\infty}^{t-x/c} n_0(t')\,\mathrm{d}t'\right]}, \\ \Delta(x,t) &= \frac{\Delta_0(x)\exp\left[-\sigma\int_0^x \Delta_0(x')\,\mathrm{d}x'\right]}{\exp\left[2\sigma c\int_{-\infty}^{t-x/c} n_0(t')\,\mathrm{d}t'\right]+\exp\left[-\sigma\int_0^x \Delta_0(x')\,\mathrm{d}x'\right]-1}. \end{aligned}\right\} \tag{11}$$

However, the CO_2 laser system is not a simple two-level system; the upper and lower levels comprise a manifold of about 15 rotational sublevels over which the available optical energy is distributed and between which optical transitions are allowed. Although the levels are discrete, they are collisionally coupled on a very fast time scale, the order of one to two collision times or about 0.2 ns at 1 atm. The amplification of pulses containing the spectrum of a single rotational transition, and which are considerably longer than this collisional relaxation time, is that of a two-level system because the reservoir of energy in the rotational manifold can communicate with the lasing transition 'instantaneously' compared with the lasing pulse time, and the two-level approximation applies.

For short optical pulses containing several rotational transitions in the so-called multiline case, the equations need to be modified to take into account the finite rational relaxation. For a simple model with an experimentally determined average rotational relaxation time between levels, τ_r, the equations on photon transport and population inversion become

$$\partial n_j/\partial t + c\,\partial n_j/\partial x = c\sigma_j \delta_j n_j, \tag{12}$$

$$\partial \delta_j/\partial t = -2\sigma_j c n_j \delta_j + (\delta_{0j} - \delta_j)/\tau_r, \tag{13}$$

$$-\partial \Delta/\partial t = -2\sum n_j c \sigma_j \delta_j. \tag{14}$$

(the summation being taken over the *lasing* levels),

$$\begin{aligned} \Delta &= N_{\text{upper, total}} - N_{\text{lower, (total)}} \\ &= \sum_{\text{upper}} N_j - \sum_{\text{lower}} N_j \end{aligned} \tag{15}$$

(the summation being taken over *all* upper and lower levels), where n_j is the specific photon density of a given transition, σ_j its stimulated emission cross section, and δ_j the jth rotational population inversion.

The instantaneous population inversion of the lasing levels, δ_j, is given by

$$\delta_j = N_{j,\text{ upper}} - N_{j,\text{ lower}}. \tag{16}$$

The equilibrium value, δ_{0j} of the rotational population inversion, i.e. the inversion that would exist without lasing is

$$\delta_{0j} = N_{j0,\text{ upper}} - N_{j0,\text{ lower}}, \tag{17}$$

$N_{j0,\ \mathrm{upper}}$, $N_{j0,\ \mathrm{lower}}$ being the equilibrium values of the respective population, without lasing. The second term on the right-hand side of (13) represents the relaxation by non-lasing levels into lasing levels to replenish the population inversion.

The parameters that determine the amplification or energy extraction from a CO_2 laser amplifier are the gain–length product, $g_0 L$, the amplifier pressure and gas mix, which sets τ_r, and the saturation energy, E_s, defined below, which depends upon the multiline content of the pulse being amplified, as well as the pressure.

For a two-level system with a square input of energy, E_i, the solution of the previous equations becomes

$$\exp\,(E_o/E_s - 1) = \exp\,(g_0 L)\,\exp\,(E_i/E_s - 1), \tag{18}$$

where E_o is the output energy.

For a two-level system with a single laser transition, E_s is given by

$$E_s = h\nu/2\sigma, \tag{19}$$

$h\nu$ being the photon energy of the transition and σ the stimulated emission cross section.

To see what this saturation energy means physically, consider a two-level system with a population inversion ΔN; the number of lasing transitions possible is $\frac{1}{2}\Delta N$, because after half the population is stimulated, the population inversion will vanish and the gain will be zero. The photon flux, ϕ_s, needed to bring this about is given simply by

$$\phi_s \sigma \Delta N = \tfrac{1}{2}\Delta N,$$

the left-hand side being the number of transitions produced by the photon flux on the population inversion and the right-hand side being the upper limit of possible transitions, or

$$\phi_s \sigma = \tfrac{1}{2}; \tag{20}$$

ϕ_s is that flux which makes the probability unity that half the upper state will be stimulated and

$$E_s = \phi_s\, h\nu. \tag{21}$$

The relation can easily be extended to CO_2, for which the input pulse may contain many rotational transitions and for which there is collisional relaxation among the lasing and non-lasing states of the upper level rotational manifold during the transit of the short pulse.

In this case, the number of states that can be stimulated consists of one-half the initial population of the lasing rotational states plus the number of non-lasing states that can collisionally relax into the lasing level during the passage of the pulse. The relaxation of these latter states into the lasing states can be represented as a restoring force, R, arising from the collisions which tend to return the lasing state population to thermal equilibrium. If n_{0j} is the value of the thermal equilibrium population of the jth lasing upper state at a given time, and n_j its instantaneous value, perturbed from n_{0j} by the lasing, then the restoring force or rate is given by

$$R = (n_{0j} - n_j)/\tau_r, \tag{22}$$

where τ_r is the average relaxation time for transfer into the jth state from all other levels. Similarly, there is relaxation out of the lower laser level during the passage of the pulse with a comparable rotational time constant. The time dependence of the population inversion from these relaxation processes are in general quite complex, but they can be calculated for the above model. For CO_2, the saturation flux can be taken as the photon flux necessary to lase

the initial population inversion augmented by the flux necessary to lase the time-dependent contribution to the lasing inversion. Detailed calculations of E_s according to Stratton (1975) for various cases are presented in figure 7.

The energy stored in the laser medium, E_{st}, is related to the small signal gain coefficient of a specific rotational transition, g_{0j}, through the equations

$$\left.\begin{aligned} E_{st} &= \tfrac{1}{2}\Delta N \langle h\nu \rangle_{\text{average}} \\ g_{0j} &= \sigma_j \delta_j = \sigma_j \chi_j \Delta N \end{aligned}\right\}, \tag{23}$$

where ΔN is the total vibrational population inversion and χ_j the partition function for the level involved. For the P(20) transition of CO_2, χ is about 6 %.

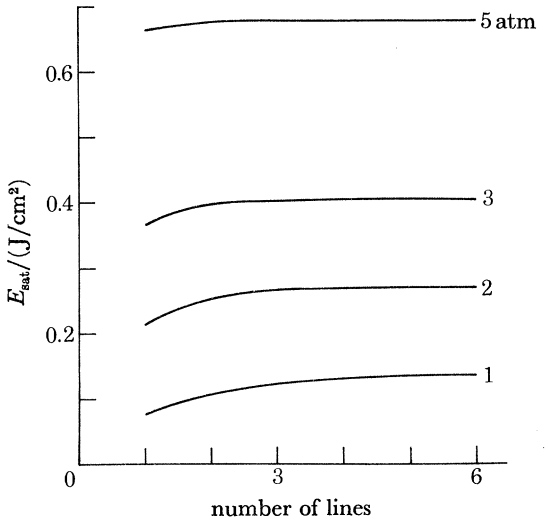

FIGURE 7. Saturation energy for 1 ns Gaussian pulses in 0 : 1 : 4 ($He : N_2 : CO_2$) gas mixture as a function of the number of rotational optical transitions in the pulse. Transitions adjacent to P(18) and P(20) are calculated, i.e. P(14), (16), (18), (20), (22) and (24). Calculated according to Stratton (1975).

The efficiency of energy extraction from an amplifier, E_0/E_{st}, as a function of $g_0 L$ and multiline content is given in figures 8 and 9 with pressure as a parameter and for an input energy equal to E_s. This efficiency levels off for $g_0 L$ values above 6 and there is a significant improvement with pressure. Above 3 atm (*ca.* 3×10^5 Pa) and with input containing three lines or more, the point of diminishing returns has been reached.

While the total energy extracted may not increase rapidly after the multiline content exceeds three transitions, the *rate* of extraction, hence, the power, can increase dramatically as more lines are included. Figure 10 illustrates this for typical operating values of large systems.

Energy-extraction efficiencies greater than 80 % have been achieved with multiline input.

6. System efficiency

The most important effect of efficiency is upon the determination of feasibility of the laser for commercial power generation. Based upon various power-plant concepts (Booth *et al.* 1976), efficiencies in the range of 5–10 % are required.

PHILOSOPHICAL TRANSACTIONS OF THE ROYAL SOCIETY A MATHEMATICAL, PHYSICAL & ENGINEERING SCIENCES

The overall system efficiency of the CO_2 laser is determined by a combination of fundamental and practical engineering factors. The ways in which fundamental parameters determine the efficiency of the CO_2 laser have been given by Leland & Kircher (1974) in a treatment that considers quantum efficiency, efficiency of excitation of the upper laser level η_e the losses by collisional deactivation from these levels during the finite pumping times ξ_m, the efficiency factor η_s arising from redistribution through molecular kinetics of the energy pumped into the upper laser level, and the efficiency for the net available extractable upper laser level energy, η_l. The various parameters have a very complex interdependence on pressure, temperature,

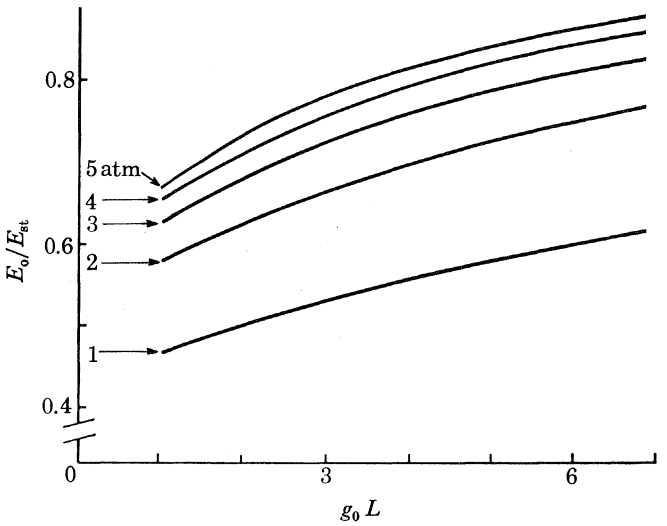

FIGURE 8. Energy extraction efficiency plotted against gain length for nanosecond input equal to the saturation flux and containing one rotational transistor (P(20)). Gas mixture is 0 : 1 : 4 ($He : N_2 : CO_2$) by volume.

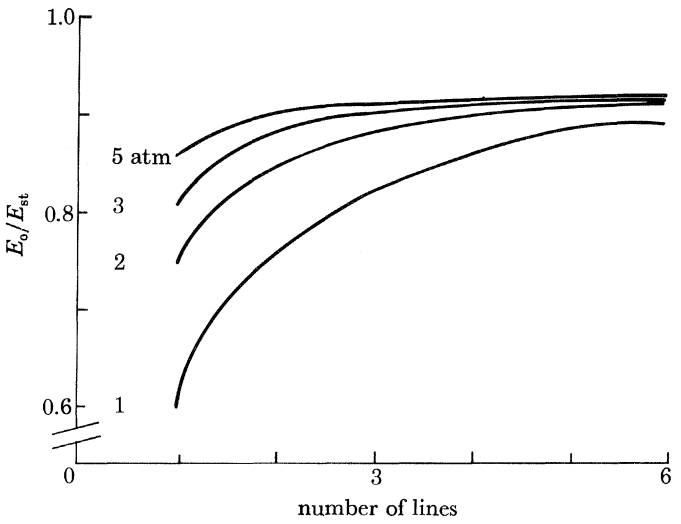

FIGURE 9. Energy extraction efficiency plotted against multiline content of input pulse. Input is a 1 ns Gaussian pulse containing the saturation flux. The gain–length product, $g_0 L$, is 6 and the gas mixture is 0 : 1 : 4 ($He : N_2 : CO_2$) by volume.

PHILOSOPHICAL TRANSACTIONS OF THE ROYAL SOCIETY A MATHEMATICAL, PHYSICAL & ENGINEERING SCIENCES

gas mix, etc., which has been treated in detail; the results are reported here. The overall fundamental efficiency for single pulse extraction is given as the product

$$\eta = \eta_e \eta_s \eta_i (1 - \xi_m)$$

and has a value of about 7%.

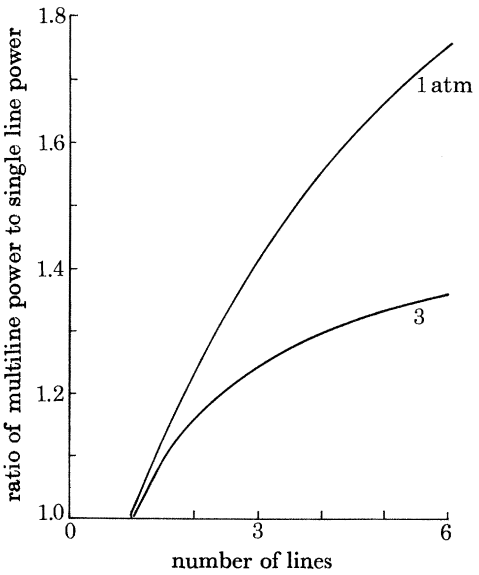

FIGURE 10. Ratio of multiline to single-line power output at $g_0 L = 6$ for a nanosecond Gaussian input pulse containing the saturation flux. Gas mixture is 0:1:4 ($He:N_2:CO_2$) by volume.

This value must now be multiplied by the practical factors to include the effects of engineering limitations, for example power supply to laser energy transfer, reflexion losses of mirrors and windows, incomplete discharge volume utilization, etc. Current estimates of these efficiency factors indicate that single-pulse efficiencies of *ca.* 5% may be achievable. Multiple-pulse schemes have been proposed (Stark *et al.* 1978) which, although complicated in practice, indicate that efficiencies of 10–20% may be possible.

Large CO_2 machines now operating at the terawatt level achieve overall electrical efficiency approaching 2%. At this size, economic trade-offs do not provide a strong incentive to do better; at the megajoule level, such consideration would influence the laser design more strongly to try to achieve efficiencies approaching 5%.

7. LARGE MACHINES

Based upon the development of CO_2 laser technology over the past decades, a succession of large CO_2 fusion lasers has been built at the Los Alamos Scientific Laboratory. Large CO_2 fusion lasers are being built in the Soviet Union and Japan. A good review of design considerations and technology for such machines has been given by Stratton (1975).

The most recent of these lasers to be brought into operation at Los Alamos is an eight-beam system, Helios, which to date has demonstrated an output of over 1500 J from a single beam with a power of more than 2 TW, so that the performance requirement has been satisfied. The manifold of eight beams has produced an output greater than 10 kJ in less than 1 ns,

PHILOSOPHICAL TRANSACTIONS OF THE ROYAL SOCIETY A MATHEMATICAL, PHYSICAL & ENGINEERING SCIENCES

with peak powers approaching 20 TW. Figure 11 shows the target chamber and the four dual beam lasers configured to provide symmetrical irradiation of laser fusion targets. This machine has been described by Ladish (1977); table 1 gives the pertinent design and performance parameters.

Helios is currently dedicated to laser target interaction experiments aimed at producing high adiabatic compressions.

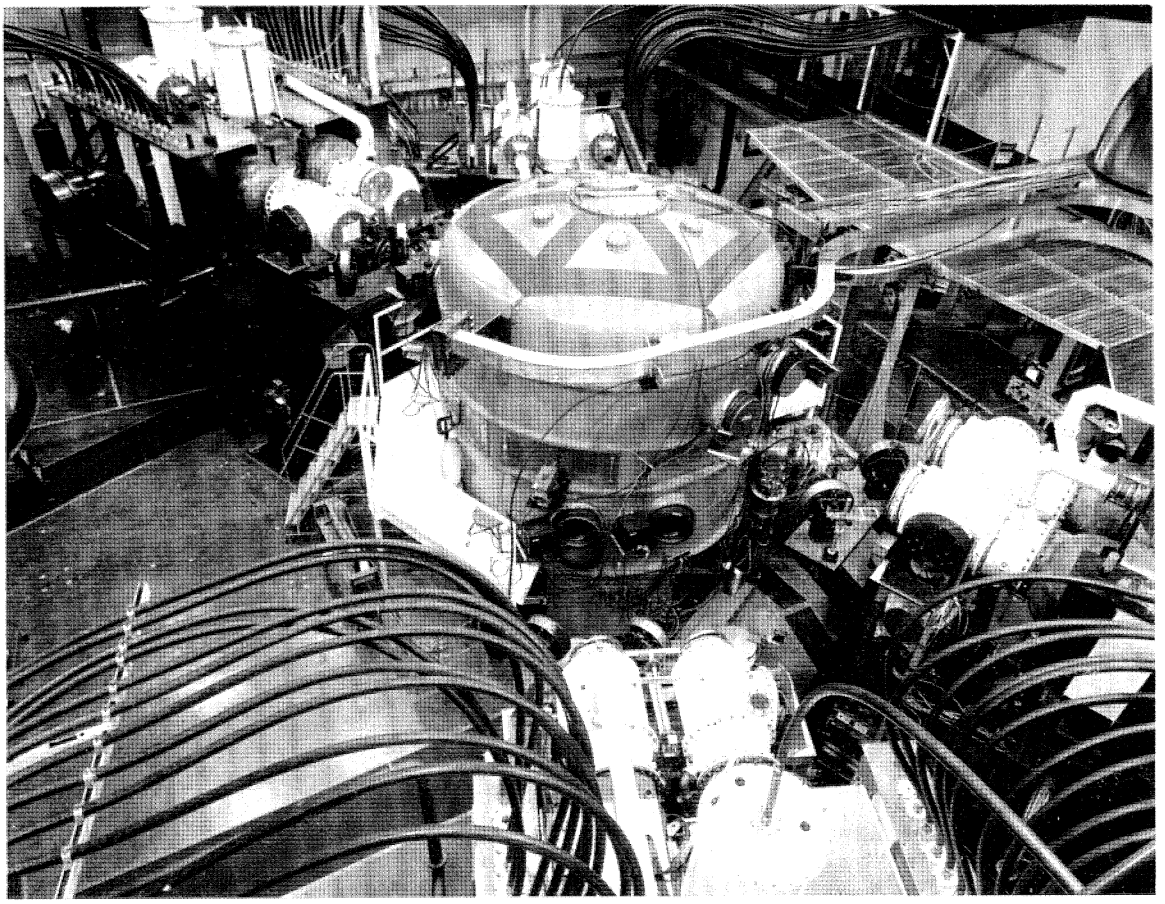

FIGURE 11. Los Alamos Helios System showing the target chamber surrounded by four dual-beam lasers. The 35 cm diameter beams enter the target chamber through the large ports, shown covered, opposite each laser amplifier.

To reach the performance range believed necessary to produce scientific breakeven, i.e. thermonuclear energy output equal to incident laser energy, a much larger machine capable of 100 kJ output energy is under design and construction. Named Antares, it will have the configuration shown in figure 12. The laser system consists of 72 laser beams arrayed in 6 annular modules of 12 beams each. The output of each beam is in excess of 1400 J in a 1 ns pulse, and at shorter pulse lengths of 0.3 ns, output powers of 100–200 TW are expected. Each of the 72 beams will have operating parameters comparable with the individual beams of the Helios. The six annular beam arrays will be brought through evacuated beam tubes to the target chamber located in another building 100 m away. This system, authorized at $54.5 M, is expected to begin operating in 1984 to investigate scientific breakeven. Stratton *et al.* (1977) gives a detailed description of this machine's design and performance.

PHILOSOPHICAL TRANSACTIONS OF THE ROYAL SOCIETY A MATHEMATICAL, PHYSICAL & ENGINEERING SCIENCES

TABLE 1. LASL HELIOS CO_2 LASER SYSTEM PARAMETERS

mechanical	
operating pressure	1800 torr (*ca.* 240 kPa)
gain volume	2 m × 35 cm × 35 cm
gas mixture	3 : 0.25 : 1 (He_2 : N_2 : CO_2)
window material	polycrystalline NaCl 40 cm diam.
electrical	
primary electron energy	280 kV
primary electron-beam current density	0.050 A/cm²
main discharge voltage	250 kV
main discharge current density	10 A/cm²
electric field strength	7 kV/cm
total main discharge current (eight beams)	640 KA
total electrical energy storage (eight beams)	600 kJ
main discharge duration	3 μs
electrical efficiency	2 %
optical	
gain coefficient, g_0	3.75 % cm^{-1}
gain–length product, g_0L	7.5
optical aperture (per beam)	900 cm²
amplifier optical configuration	triple pass
output pulse duration	< 1 ns (f.w.h.m.)
output energy per beam design	1250 J (1500 J attained)
final amplifier input energy	0.1 J
total g_0L (three passes)	22.5

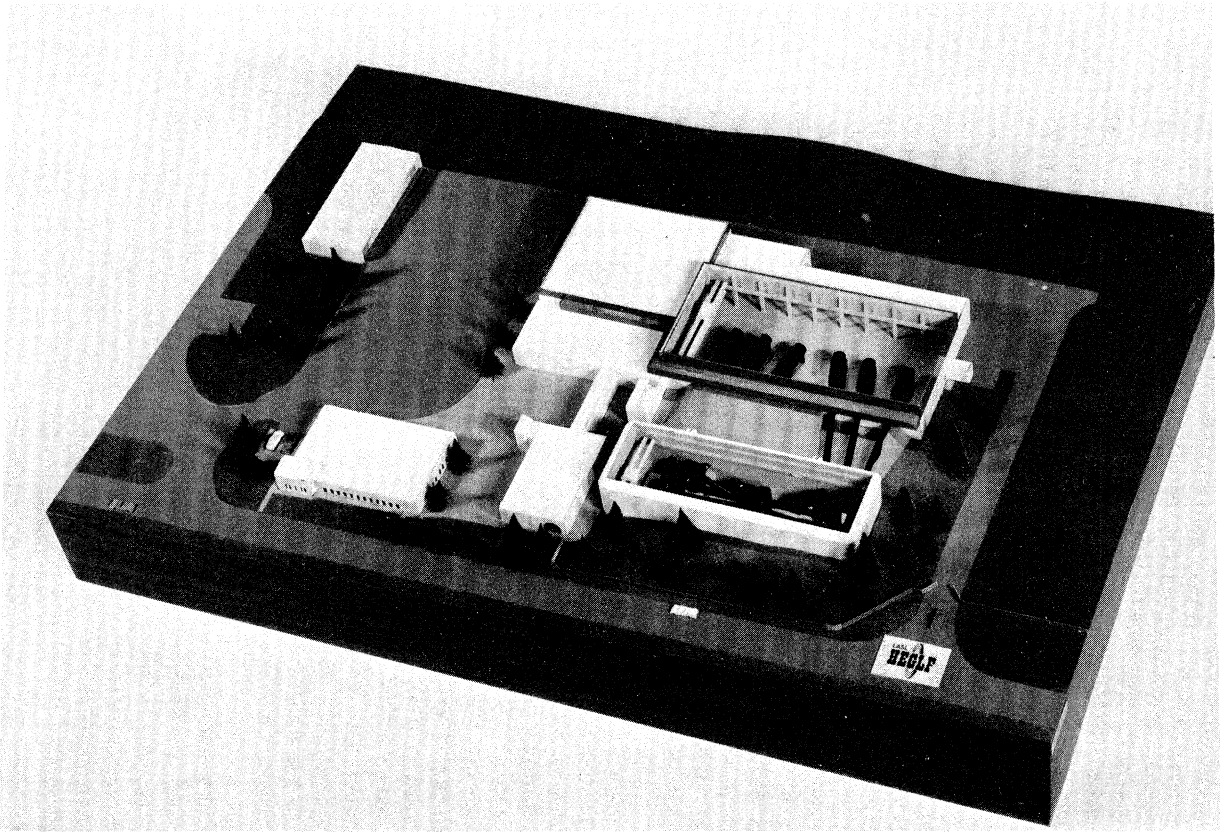

FIGURE 12. Laser facility and target building configuration for the 100 kJ Antares laser. Operation is planned for 1984.

PHILOSOPHICAL TRANSACTIONS OF THE ROYAL SOCIETY A MATHEMATICAL, PHYSICAL & ENGINEERING SCIENCES

As a result of the experience with these large machines, CO_2 fusion laser technology has matured so that the design of even larger machines in a megajoule range can be undertaken with confidence. Fusion lasers at the megajoule level are expected to produce pellet gains, the ratio of energy out to energy incident, in the range of 100. Such performance could be available within a decade.

8. Conclusion

The laser performance requirements for fusion set forth in this article are clearly met by high-energy, short-pulse CO_2 lasers, and a fusion programme based on their use is under way at Los Alamos. The ability of the CO_2 laser, or for that matter, of any laser to compress and heat a plasma to the requisite densities and temperatures, remains to be demonstrated. Previously it was believed that the long wavelength of the CO_2 laser represented a fundamental obstacle with regard to these processes because of critical density considerations which scaled as the square of the wavelength. Recent experimental and theoretical work have modified this view by taking into account the physics of the electromagnetic pressure. When this is included, the absorption and transport processes in the plasma appear to be modified in the direction of greatly reduced wavelength sensitivity.

The reader should be aware that notwithstanding the healthy optimism of the total programme, the road to scientific breakeven is likely to be a long and difficult one: the history of the magnetic fusion programme supports such a view. The understanding of the physical processes at any wavelength is far from complete and many difficult problems are yet to be recognized. Although no fundamental obstacles have yet been identified to the use of CO_2 lasers for fusion, questions on the wavelength dependence of energy absorption and transport, adiabatic compression, and instabilities, to cite a few areas, will certainly need much more experimental investigation at all laser wavelengths before the feasibility can be established with confidence. The CO_2 laser facilities planned will allow this investigation. If all goes well, we can expect feasibility demonstrations, i.e. scientific breakeven, in the mid-1980s with the CO_2 laser, and the way would be cleared to proceed to the next difficult problem, commercial application.

The potential benefits from laser fusion are so great that a vigorous, optimistic programme is justified. The CO_2 laser provides an important capability in this quest.

The present status of CO_2 laser technology has resulted from the efforts of the staff and support members of the Laser Research and Technology Division of the Los Alamos Scientific Laboratory. The work was performed under the auspices of the U.S. Department of Energy.

References (Fenstermacher)

Basov, N. G., Belenov, E. M., Danilychev, V. A. & Suchkov, A. F. 1975 *Soviet Phys. Usp.* **17**, 705–721.
Booth, L. A., Freiwald, D. A., Frank, T. G. & Finch, F. T. 1976 *Proc. Inst. elect. Electron. Engrs* **64**, 1460.
Daugherty, J. D., Pugh, E. R. & Douglas-Hamilton, D. H. 1972 *Bull. Am. phys. Soc.* **17**, 399.
De Maria, A. J. 1976 In *Principles of laser plasmas* (ed. G. Bekefi), ch. 8, pp. 315–368. New York: Wiley.
Fenstermacher, C. A., Nutter, M. J., Rink, J. P. & Boyer, K. 1971 *Bull. Am. phys. Soc.* **16**, 42.
Fenstermacher, C. A., Nutter, M. J., Leland, W. T. & Boyer, K. 1972 *Appl. Phys. Lett.* **20**, 56–60.
Frantz, L. M. & Nodvik, J. S. 1963 *Appl. Phys.* **34**, 2346–2349.
Kryukov, P. G. & Letokhov, V. S. 1970 *Soviet Phys. Usp.* **12**, 641–672.
Ladish, J. S. 1977 The CO_2 laser fusion effort at Los Alamos Scientific Laboratory. *Los Alamos Scientific Laboratory Report* no. LA-UR-77-1165.

Leland, W. T. 1976 Relation of electric discharge parameters to short-pulse laser efficiency. *Los Alamos Scientific Laboratory Report.* no LA-UR-75-1035; and (in Russian) *Kvantovaya Electronika* **3**, 855–863.
Leland, W. T. & Kircher, M. 1974 The relation of CO_2 discharge kinetics to the efficiency of short-pulse amplifiers. *Los Alamos Scientific Laboratory Report* no. LA-UR-74-637.
Moore, C. B., Wood, R. E., Hu, B.-L. & Yardley, J. T. 1967 *J. chem. Phys.* **36**, 4222–4321.
Schappert, G. T. 1973 *Appl. Phys. Lett.* **23**, 319.
Stark, E. E., Leland, W. T. & Volkin, H. C. 1978 Nanosecond pulse amplification in CO_2 at efficiencies exceeding 20%. Paper no. WC-14, programme, Inertial Confinement Fusion Topical Meeting, *I.E.E.E./O.S.A.*, San Diego.
Stratton, T. F. 1975 In *High power gas lasers* (*Conference Series* no. 29) (ed. E. R. Pike), pp. 284–311. Bristol and London: The Institute of Physics.
Stratton, T. F., Durham, F. P., Jansen, J., Leland, W. T., Reichelt, W. H. & Zeigner, V. L. 1977 The LASL 100 kJ CO_2 laser for ICF research: Antares. Paper no. TuC7–1, programme, Inertial Confinement Fusion Topical Meeting, *I.E.E.E./O.S.A.*, San Diego.
Walsh, T. E. 1966 *RCA Rev.* pp. 323–335.
Witteman, W. J. 1966 *Philips Res. Rep.* **21** (2), 73–84.

Discussion

C. Yamanaka (*Institute of Laser Engineering, Osaka University, Japan*). The parasitic oscillation of the CO_2 laser system is a very crucial problem. How can the oscillation in full power operation be prevented?

The distance between the laser and the target is only 10 m, which introduces this kind of trouble.

C. Fenstermacher. There are two sources of parasitics for any large laser system: those internal to the amplifier system and those resulting from interaction with the target system. The first source of parasitics, i.e. the feedback paths entirely within the amplifier system, have been successfully treated with saturable, gaseous absorber cells placed within the amplifiers. These have operated up to and above all the design conditions at which large CO_2 laser systems are envisioned to operate, that is, g_0L (gain–length values) between 7 and 8, and output energies per single beam of about 1500 J. Thus, the parasitic oscillation from this source appears to be well solved.

Secondly, the problem of interaction with the target is a more difficult one to handle. If the solution were sought through gaseous saturable absorbers, it would place great demands upon such absorbers because they must be in the output beam to provide the appropriate small signal attenuation to suppress the parasitic, and at the same time have exceedingly high transmission, the order of 95% or above, to be economical. Fortunately, a second solution can be found for such parasitic problems that relies on the fact that the pumping time for CO_2 high-pressure laser systems can be the order of 1–2 μs. For large-scale systems, the type sought in laser fusion, the laser–target facility scale is such that the round-trip time for parasitic build up between the target and some amplifier reflecting element is long compared with the pump time; thus, the gain does not exist in this parasitic path sufficiently long for the parasitic oscillation to build up. This has been verified by calculations, and represents the type of target isolation that would be used in the Antares 100 TW laser system. In the current systems, such as in the Gemini 10 TW system, designed long before there was a good appreciation of such problem, this 10 m distance between the target chamber and laser facility is inadequate to use this mechanism. However, through the careful selection of saturable absorbers for this system, it is expected that approximately 80%, and possibly more, depending upon the results of ongoing investigations, of the output energy will be able to be brought on target.

PHILOSOPHICAL TRANSACTIONS OF THE ROYAL SOCIETY A MATHEMATICAL, PHYSICAL & ENGINEERING SCIENCES

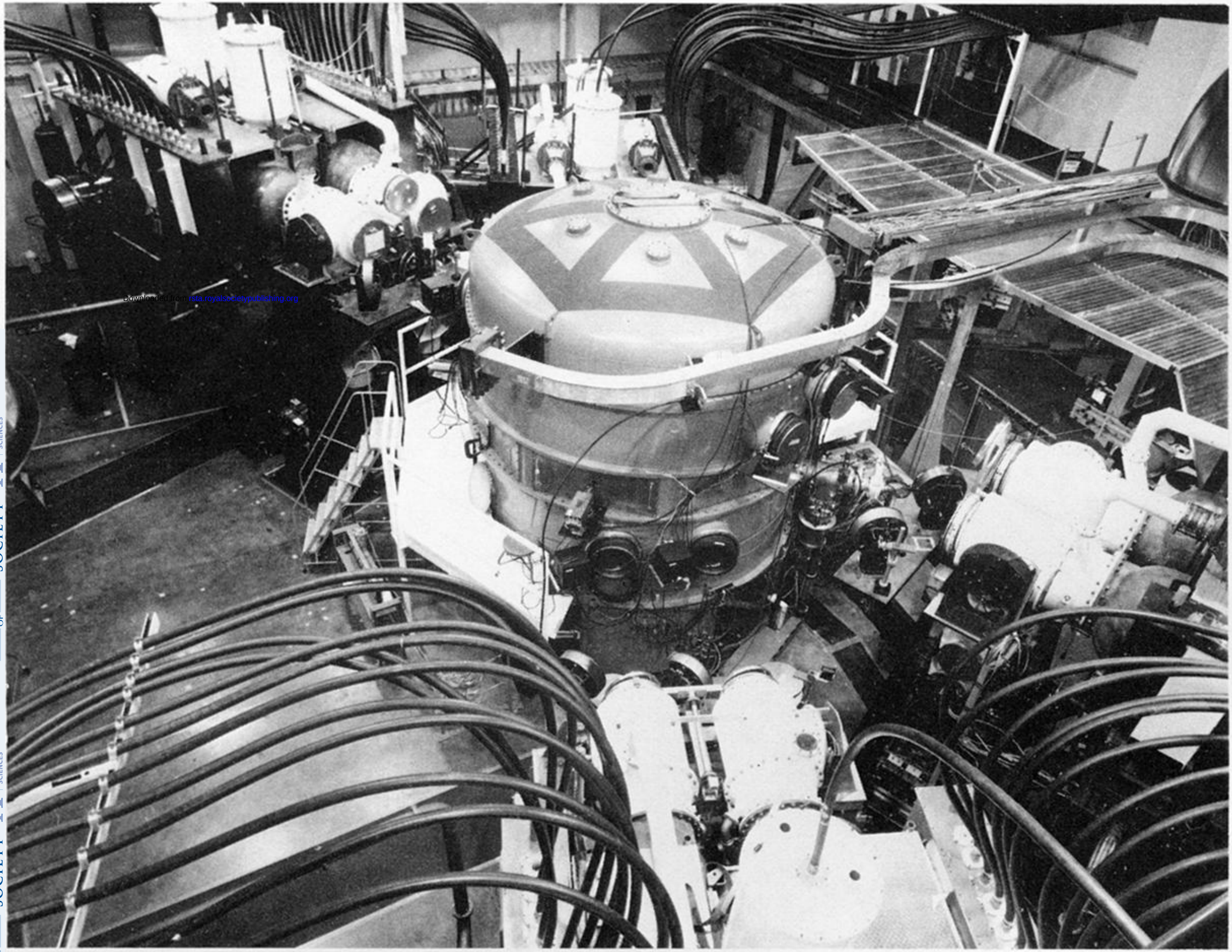

FIGURE 11. Los Alamos Helios System showing the target chamber surrounded by four dual-beam lasers. The 35 cm diameter beams enter the target chamber through the large ports, shown covered, opposite each laser amplifier.

PHILOSOPHICAL TRANSACTIONS OF THE ROYAL SOCIETY A MATHEMATICAL, PHYSICAL & ENGINEERING SCIENCES

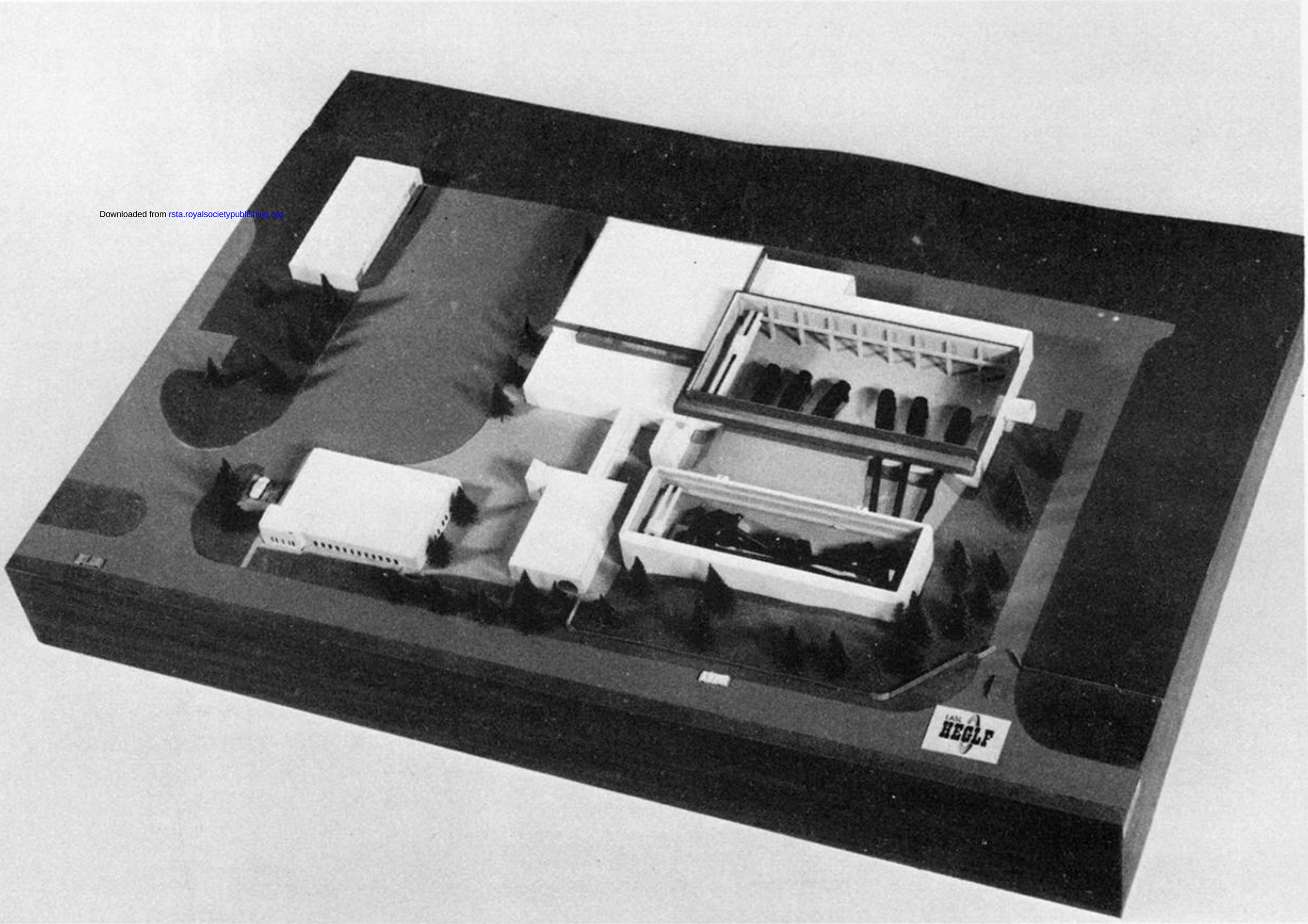

FIGURE 12. Laser facility and target building configuration for the 100 kJ Antares laser. Operation is planned for 1984.

PHILOSOPHICAL TRANSACTIONS OF THE ROYAL SOCIETY A MATHEMATICAL, PHYSICAL & ENGINEERING SCIENCES